


Functional Analysis of Induced Human Ballooned Hepatocytes in a Cell Sheet-Based Three Dimensional Model

Botao Gao^{1,2} · Katsuhisa Sakaguchi³ · Tetsuya Ogawa⁴ · Yuki Kagawa⁴ · Hirosugu Kubo⁴ · Tatsuya Shimizu² 

Received: 4 June 2020/Revised: 22 August 2020/Accepted: 26 August 2020/Published online: 30 January 2021
© The Korean Tissue Engineering and Regenerative Medicine Society 2021

Abstract

BACKGROUND: Ballooned hepatocytes (BH) are a key histological hallmark of nonalcoholic steatohepatitis (NASH), yet their consequences for liver-specific functions are unknown.

METHODS: In our previous study, an experimental model of human induced-BHs (iBH) has been successfully developed based on cell sheet technology. This study aimed to determine the functions of iBHs in the primary human hepatocyte/normal human dermal fibroblast (PHH/NHDF) co-culture cell sheets. Normal hepatocytes in the PHH/3T3-J2 co-culture cell sheets were set as a control, since 3T3-J2 murine embryonic fibroblasts have exhibited previously long term maintenance of PHH functions.

RESULTS: It was found that, albumin secretion was not affected in iBHs, but urea synthesis as well as cytochrome P450 enzyme (CYP) activities including CYP1A2 and CYP3A4, were significantly reduced in iBHs. Besides, loss of bile canaliculi was observed in iBHs. These findings are consistent with clinical studies of human NASH. In addition, PHH/NHDF cell sheets demonstrated two fold higher TGF- β 1 secretion compared with PHH/3T3-J2 cell sheets. Furthermore, treatment with a TGF- β inhibitor and a semi-synthetic bile acid analogue (obeticholic acid, phase 3 trial of NASH therapy) ameliorated the histological appearance of established iBHs.

CONCLUSION: In summary, this study demonstrates the priority of iBHs in recapitulating not only histology but also clinically relevant hepatic dysfunctions in human NASH and suggests TGF- β and bile acid related signal pathway may play important roles in the formation of iBHs.

Keywords Cell sheet · Ballooned hepatocytes · Liver function · NASH

✉ Tatsuya Shimizu
shimizu.tatsuya@twmu.ac.jp

¹ Guangdong Key Lab of Medical Electronic Instruments and Polymer Materials Products, National Engineering Research Center for Healthcare Devices, Guangdong Institute of Medical Instruments, Guangdong Academy of Sciences, Guangzhou 510550, China

² Institute of Advanced Biomedical Engineering and Science, Tokyo Women's Medical University, TWIns, 8-1 Kawada-cho, Shinjuku-ku, Tokyo 162-8666, Japan

³ Department of Integrative Bioscience and Biomedical Engineering, Graduate School of Advanced Science and Engineering, Waseda University, TWIns, 2-2 Wakamatsu-cho, Shinjuku-ku, Tokyo 162-8480, Japan

⁴ Ogino Memorial Laboratory, Nihon Kohden Corporation, TWIns, 8-1 Kawada-cho, Shinjuku-ku, Tokyo 162-8666, Japan

1 Introduction

In the past few decades, nonalcoholic fatty liver disease (NAFLD) has become an urgent public health problem worldwide [1–3]. NAFLD consists of a spectrum of liver diseases ranging from simple fatty liver (steatosis) to the nonalcoholic steatohepatitis (NASH). NASH is a more severe disease, which increases the risk of cirrhosis and primary hepatic carcinoma. However, the development and progression of NASH is not entirely understood.

Mounting evidence has suggested that abnormal changes in liver-specific functions may promote NASH development. It has been demonstrated that NASH patients have a functional reduction in the capacity for ureagenesis and the resulted accumulation of ammonia can lead to fibrosis development, increasing the risk of disease progression [4]. Several studies have shown that NASH patients have increased rates of bile acid synthesis [5, 6]. Importantly, they have demonstrated that bile acids levels correlate with markers of hepatic injury, such as steatosis, ballooning and fibrosis, suggesting a possible role for bile acids in the progression of NASH.

Drug metabolism in the liver are also affected by NASH. Cytochrome P450 (CYP) 3A4 is responsible for the oxidative metabolism of more than 50% of all drugs. It has been found that, CYP3A4 activity is decreased in NASH patients [7], which might be due to inflammatory cytokines, such as TGF β 1 [8]. TGF β 1 has been reported to induce apoptosis in various epithelial cells at high concentrations [9] and also participates in NASH through regulation of cell death and lipid metabolism in a mouse model [10].

Effects of NASH on protein synthesis in the liver are complicated. It has been found that NASH patients show reduced synthesis of apolipoprotein B-100, increased synthesis of fibrinogen and unchanged synthesis of albumin when compared with healthy controls [11]. Additionally, some pioneering studies demonstrate that sonic hedgehog (SHH), which is secreted by ballooned hepatocytes (BH), is increased in NASH and its activation parallels histologic severity of hepatic injury [12, 13].

Hepatocellular ballooning is a key histological hallmark of NASH. It is associated with the liver inflammation and fibrosis [14–16] and used to score disease severity [17]. Comprehensive study of BHs will help us to better understand NASH pathogenesis, but still little is known about BHs due to the lack of appropriate experimental models. In particular, as far as we know, no study to date has systematically quantified the liver-specific functions of BHs *in vitro*.

Our lab has been focusing on cell sheet based-tissue engineering. “Cell sheet” is a confluent mono-layer of cells

harvested from an innovative temperature-responsive cell culture plates (TRCP) by reducing temperature [18, 19]. In our previous study, primary human hepatocytes (PHH), which are considered as the gold standard of *in vitro* human liver model were co-cultured with normal human dermal fibroblasts (NHDF) on TRCPs and harvested as contracted co-culture cell sheets. Interestingly, BHs were reproduced in this cell sheet-based *in vitro* three dimensional (3D) model [20]. Similar to BHs in NASH livers, the induced BHs (iBH) display cell enlargement, fat accumulating, rarefied cytoplasm, mitochondrial dysfunction, endoplasmic reticulum (ER) stress, increased secretion of SHH and so on. Although high glucose/high insulin media and NHDF dependent stimulation are associated with occurrence of iBHs, further mechanism is not clear.

We hypothesized that liver-specific functions, such as albumin secretion, urea synthesis, cytochrome P450 (P450) enzyme activities and bile canaliculi network formation were altered in iBHs relative to normal hepatocytes. Therefore, the main purpose of this study was to investigate liver-specific functions of iBHs and explore their possible pathogenesis.

2 Materials and methods

2.1 Fibroblast culture

NHDF(Lonza, Basel, Switzerland) were cultured in high-glucose Dulbecco's Modified Eagle's Medium (DMEM, Corning, NY, USA) supplemented with 10% fetal bovine serum (FBS; Thermo Fisher Scientific, Waltham, MA, USA) and 1% penicillin–streptomycin and cultured at 37 °C in a humidified atmosphere with 5% CO₂. After passage on stiff tissue culture plastic in serum supplemented culture media, NHDFs are activated and display aligned, dense actin stress fibers [20]. Activated NHDFs were used for co-culture with PHHs in cell sheets to induce hepatocellular ballooning.

3T3-J2 murine embryonic fibroblasts (Kerafast, Boston, MA, USA) were cultured in high-glucose DMEM supplemented with 10% bovine calf serum (GE Healthcare, Little Chalfont, UK) and 1% penicillin–streptomycin (Corning) and cultured at 37 °C in a humidified atmosphere with 5% CO₂. 3T3-J2 fibroblasts, which are irradiated 3T3 fibroblasts, are not easy to be activated after passage on stiff tissue culture plastic. They reveal random, relatively sparse actin stress fibers [20]. Khetani et al. have done a lot of great work, demonstrating that 3T3-J2 fibroblasts are superior in maintaining liver-specific functions compared to other non-parenchymal cells [21–23]. They have found that 3T3-J2 fibroblasts express diverse molecules present in the liver, such as decorin [21] and T-cadherin [24], both of which contribute to maintaining functions in hepatocytes

from different species. Therefore, co-culture of PHHs and 3T3-J2 fibroblasts in cell sheets is used as a positive control to assess liver-specific functions of iBHs in the PHH/NHDF co-culture cell sheets.

2.2 PHH/fibroblast co-culture

PHHs and fibroblasts were co-cultured on collagen 1 coated 24 well TRCPs (UpCell; CellSeed, Tokyo, Japan) by a previously reported method [20]. In brief, cryopreserved-PHHs (Thermo Fisher Scientific, Lot: Hu1652 and Hu8200_A) were firstly seeded at 1×10^5 cells/well. On the next day, 3T3-J2 fibroblasts (3×10^5 cells/well) and NHDFs (2×10^5 cells/well) were seeded, respectively. Then the co-cultured cells were cultured for 3 days until harvesting at 37 °C in a humidified atmosphere with 5% CO₂. The co-culture media was composed of high-glucose DMEM supplemented with 0.1 μM dexamethasone (Sigma Aldrich, St. Louis, MO, USA), 1% ITS premix (insulin/human transferrin/selenous acid and linoleic acid; Corning), 0.2 μM glucagon (Sigma Aldrich), 10% FBS, 1% Penicillin–streptomycin.

2.3 Harvest and culture of PHH/fibroblast co-culture cell sheets

On day 0, confluent co-cultured PHHs and fibroblasts on 24 well TRCPs were incubated at 20 °C for 30–60 min. Then these cells detached, shrank and formed tightly-packed multilayered cell sheets.

The contracted PHH/fibroblast co-culture cell sheets were transferred into collagen 1-coated 35 mm polystyrene cell culture dishes (IWAKI, Tokyo, Japan) and incubated at 37 °C without media for adherence of cell sheets. After 10–20 min, 1 ml co-culture media were added. The cell sheets were cultured for 3 weeks with daily media change.

2.4 Drug treatments

From day 11, PHH/NHDF cell sheets were exposed to DMSO vehicle control (Sigma Aldrich), 10 μM obeticholic acid (AdipoGen Life Sciences, Basel, Switzerland), or 10 μM TGF-β inhibitor (SB505214; Sigma Aldrich) until day 21.

2.5 Enzyme-linked immunosorbent assay (ELISA) analysis

At pre-determined time points, cell culture supernatants over a 24 h period were collected and stored at –30 °C until assayed. Albumin secretion was detected by human albumin enzyme-linked immunosorbent assay (ELISA) quantitation kit (Bethyl Laboratories, Montgomery, TX,

US). Urea synthesis was determined using a colorimetric assay kit (BioChain, Newark, CA, USA). The amount of TGF-β1 ligands was determined by human TGF-β1 ELISA kit (Thermo Fisher Scientific). Measurements were performed in 3 independent experiments. In each experiment, replicate samples were more than 3.

2.6 CYP enzyme activities

On day 11, PHH/NHDF cell sheets and PHH/3T3-J2 cell sheets were washed with PBS and Williams' E medium (Thermo Fisher Scientific). Then Williams' E medium containing 100 μM phenacetin (PHE; Sigma Aldrich) and 50 μM midazolam (MDZ; Sigma Aldrich) were added. PHE and MDZ were substrate of CYP1A2 and CYP3A4, respectively. PHHs metabolized two CYP substrates and released their metabolites into culture media. After 10 min incubation, 20 μl cell culture supernatants were collected. They contained metabolites of PHE and MDZ, which were acetaminophen and hydroxymidazolam, respectively. The two metabolites were measured by API 5000 LC/MS/MS System (AB applied biosystems, Foster City, CA, USA). Biotransformation rate of CYP substrates into specific metabolites was used to indicate CYP enzyme activities. Measurement of CYP activities was performed in 3 independent experiments. In each experiment, replicate samples were more than 3.

2.7 Bile canaliculi staining

On day 11, PHH/NHDF cell sheets and PHH/3T3-J2 cell sheets were washed with PBS for 3 times, and incubated at 37 °C for 10 min in 2 μg/ml of 5-(and-6)-carboxy-20,70-dichlorofluorescein diacetate (CDFDA; Sigma Aldrich) in DMEM without phenol red. Then, cell sheets were washed 3 times with PBS and imaged with a fluorescence microscope (Nikon, Tokyo, Japan).

2.8 Hematoxylin and eosin staining

On day 11 and day 21, cell sheet samples were fixed in 4% paraformaldehyde at room temperature for 1 h. Fixed cell sheets were embedded in paraffin, sliced into 4 μm sections, and deparaffinized for standard histological staining with hematoxylin and eosin (HE).

2.9 Immunofluorescence staining

In brief, paraffin-embedded sections were incubated with primary antibody of E-cadherin (Abcam, Cambridge, UK) and vimentin (Abcam). Alexa Fluor 488 goat anti-rabbit and Alexa Fluor 594 goat anti-mouse were used as secondary antibodies for fluorescence staining. The cell nuclei

were stained with 4', 6-diamidino-2-phenylindole (DAPI). Finally, the sections were mounted, dried and imaged with a fluorescence microscope (Nikon).

2.10 Statistical analysis

The results were expressed as mean \pm standard deviation (SD) values. Significant differences between two groups were tested using Student's *t* test. Values of $*p < 0.05$ were considered statistically significant.

3 Results and discussion

3.1 iBHs display unaffected albumin secretion

As shown in Fig. 1A, iBHs continued to secrete albumin during the 10 days culture and no significant differences in secreted albumin could be observed between iBHs in PHH/NHDF cell sheets and normal hepatocytes in PHH/3T3-J2 cell sheets on both day 4 ($*p = 0.79$) and day 10 ($*p = 0.08$), which suggests that albumin secretion is unaffected in iBHs. This result is consistent with a clinical study which demonstrates that NASH patients have unchanged serum albumin relative to healthy people [11].

We speculate that a stress-responsive signaling pathway called the unfolded protein response (UPR) activated by endoplasmic reticulum (ER) stress may explain the current result. UPR is able to relieve ER stress and do not affect ER export and secretion of some proteins [25]. For example, Bartalena et al. have found that tunicamycin-induced ER stress does not inhibit the albumin secretion from human hepatoma Hep G2 cells [26]. Further, Ota et al. suggest effect of tunicamycin-induced ER stress on albumin secretion is dependent on magnitude of ER stress [27]. They have found that modest ER stress does not inhibit the albumin secretion in rat hepatoma McA-RH7777 cells, whereas excessive ER stress reduce the albumin secretion. Previously, we have demonstrated presence of ER stress in iBHs [20], and thus it is reasonable to assume that unaffected albumin secretion from iBHs may be attributed to modest ER stress.

3.2 iBHs display reduced urea synthesis

Although iBHs in PHH/NHDF cell sheets showed a reduction tendency of urea synthesis compared to PHH/3T3-J2 cell sheets on day 4, there were no significant differences ($*p = 0.11$) (Fig. 1B). However, significant differences were found on day 10 ($*p < 0.05$) (Fig. 1B),

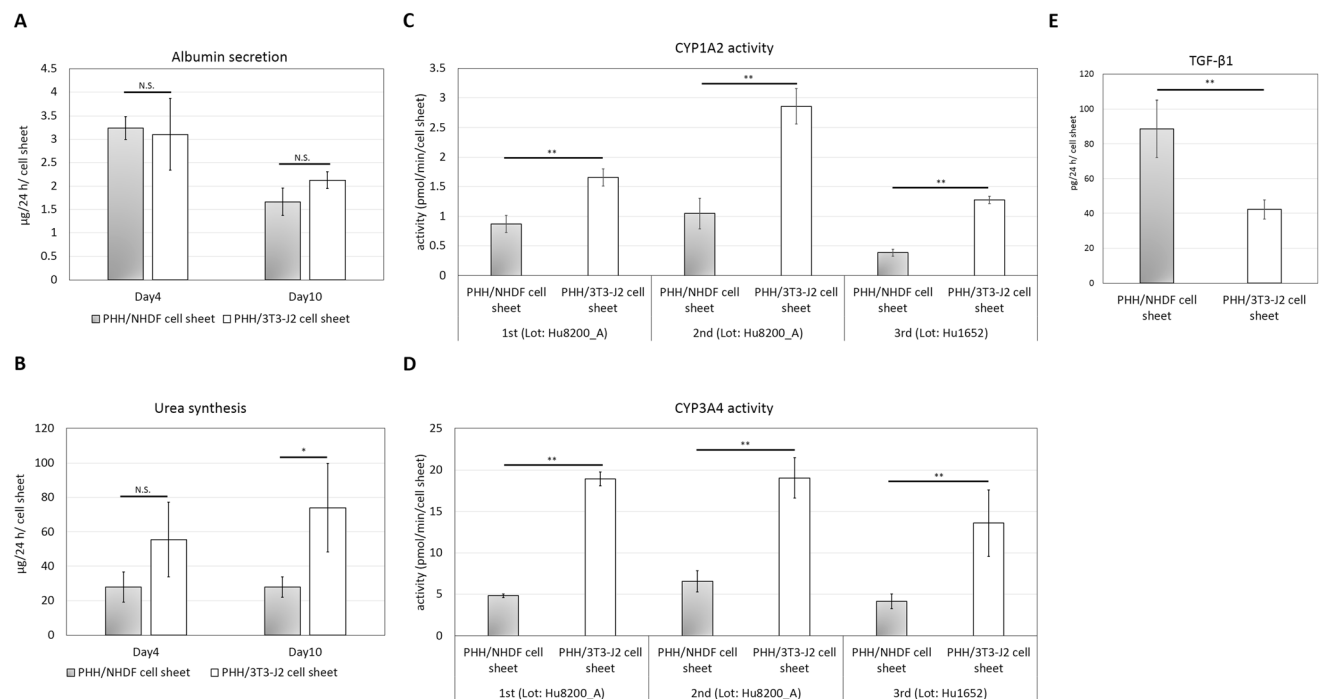


Fig. 1 Liver-specific functional analysis of iBHs in PHH/NHDF cell sheets and normal hepatocytes in PHH/3T3-J2 cell sheets. **A** Albumin secretion on day 4 and day 10. **B** Urea synthesis on day 4 and day 10. **C** CYP1A2 activities on day 11. **D** CYP3A4 activities on day 11. **E** TGF- β 1 secretion on day 4. Measurements of albumin, urea and TGF- β 1 were performed in three independent experiments using one

lot of PHHs (Hu8200_A). Measurements of CYP activities were performed in three independent experiments using two lots of PHHs (Hu8200_A \times 2 + Hu1652 \times 1). In each experiment, more than three replicate samples were measured. $*p < 0.01$, $*p < 0.05$, N.S. no significant difference

suggesting that urea synthesis by iBHs was partially suppressed. This result may be explained by a reduction in the expression of urea cycle enzymes (UCE) in NASH patients [28]. Normally, UCEs convert toxic nitrogen waste into urea, thus dysregulation of UCEs leads to the impairment of urea synthesis and accumulation of ammonia, which is toxic and increases the risk of disease progression.

Thomsen et al. suggest severe mitochondrial dysfunction seems to be the dominant cause of progressive reduction of UCEs in an experimental NASH model [4]. In agreement with this concept, we have observed the enlarged mitochondria and intramitochondrial crystals in iBHs [20], which suggests the presence of mitochondrial dysfunction and thus may contribute to reduced urea synthesis in iBHs.

3.3 iBHs display reduced CYP activities

Incubation of cell sheets with PHE and MDZ resulted in the appearance of the CYP1A2 metabolite, acetaminophen and CYP3A4 metabolite, hydroxymidazolam in the culture media. The levels of acetaminophen and hydroxymidazolam in the PHH/NHDF cell sheets were significantly lower than PHH/3T3-J2 cell sheets in three independent experiments on day 11 (Fig. 1C, D), suggesting reduced CYP1A2 and CYP3A4 activities in iBHs. These findings align with a previous study of clinical samples from NAFLD patients, which has shown a significant decrease in hepatic CYP1A2 and CYP3A4 activities in NASH patients when compared with healthy people [29]. In another study, CYP3A4 activity was directly examined in biopsy-proven NASH patients and decreased *in vivo* CYP3A4 activity is also found [7].

It has been reported that decreased CYP activities may be attributed to TGF- β 1 [8, 30], which can be secreted by activated fibroblasts or hepatic stellate cells. Inspired by these studies, we measured secretion of TGF- β 1 and found PHH/NHDF cell sheets exhibited two fold higher TGF- β 1 secretion than PHH/3T3-J2 cell sheets (Fig. 1E), suggesting a possible reason for decreased CYP activities in iBHs.

3.4 iBHs display loss of bile canaliculi

On day 11, phase contrast images show many rounded iBH clumps in PHH/NHDF cell sheets (Fig. 2A), whereas normal hepatocytes in PHH/3T3-J2 cell sheets displayed flattened and prototypical hepatic morphology, such as polygonal shape, distinct nuclei/nucleoli, and demarcated cell–cell borders (Fig. 2B). Furthermore, CDFDA staining image reveals connective bile canaliculi networks in PHH/3T3-J2 cell sheets (Fig. 2D). In contrast, a significant loss of bile canaliculi was observed in PHH/NHDF cell sheets (Fig. 2C).

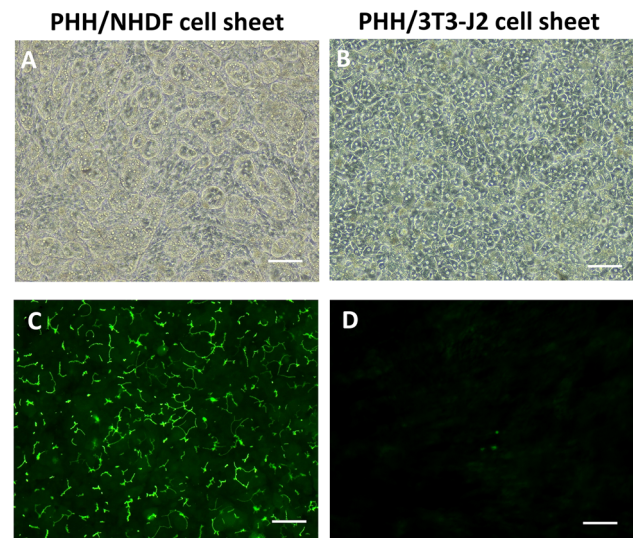


Fig. 2 Bile canaliculi network formation of iBHs in PHH/NHDF cell sheets and normal hepatocytes in PHH/3T3-J2 cell sheets. **A, B** Phase contrast images, **C, D** transport of fluorescent CDFDA (green) to the apical (canalicular) domain of PHHs showed bile canaliculi network. Scale bar represents 100 μ m

This finding corresponds to an excellent study done by Segovia-Miranda et al. [31]. They analyze human liver tissues from NAFLD patients at different stages by using multiphoton imaging, 3D digital reconstructions and computational simulations. For the first time, they report morphological defects of bile canaliculi and a strong reduction in the total length and branches crossing regions of the bile canaliculi in the early stage of NASH. They also indicate presence of increased biliary pressure and microcholestasis in NASH, which is consistent with elevated cholestatic biomarkers in patients' sera.

To further investigate the cause of loss of bile canaliculi in PHH/NHDF cell sheets, immunofluorescence staining of E-cadherin/vimentin was done. As shown in Fig. 3A, B, PHHs in both of PHH/NHDF cell sheets and PHH/3T3-J2

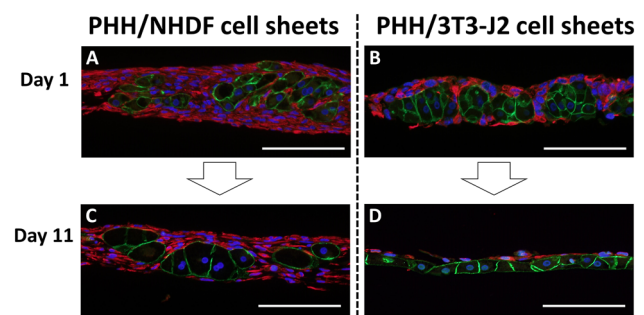


Fig. 3 Immunofluorescent staining of E-cadherin (green) and vimentin (red) to observe PHH and fibroblast respectively. Representative fluorescent images of **A, C** PHH/NHDF cell sheets and **B, D** PHH/3T3-J2 cell sheets on **A, B** day 1, **C, D** day 11 were shown. Scale bar represents 100 μ m

cell sheets formed 3D aggregations, which were surrounded by fibroblasts on day 1. However, the PHH aggregations were not observed on day 11 in PHH/3T3-J2 cell sheets. Instead, stratified structure of PHH layer and 3T3-J2 layer were observed (Fig. 3D). The intact, flattened layer of PHHs allows wide, close PHH–PHH contacts, thus may contribute to the connective bile canaliculi network formation in PHH/3T3-J2 cell sheets. This cell segregation of PHH and 3T3-J2 indicates collective cell migration and may be caused by specific cadherin expression of PHHs (E-cadherin) and 3T3-J2 fibroblasts (T-cadherin) [24].

However, this cell segregation process was not observed in PHH/NHDF cell sheets on day 11 (Fig. 3C). Instead, hepatocellular ballooning was observed in PHH/NHDF cell sheets. We speculate that excessive deposition of extracellular matrix (ECM) produced by activated NHDFs may inhibit cell migration and reorganization, thus PHHs are locked in the fibrous-like tissues and cannot move to form bile canaliculi network, which may lead to micro-cholestatics and even iBH formation.

To prove this hypothesis, we used TGF- β inhibitor to suppress ECM production since TGF- β 1 was highly found in PHH/NHDF cell sheets (Fig. 1E). We also applied a semi-synthetic bile acid analogue—obeticholic acid, which is undergoing clinical trial of NASH therapy [32], to control the possible micro-cholestatics in iBHs.

3.5 TGF- β inhibitor or obeticholic acid ameliorates the histological appearance of established iBHs

SB505124 (TGF- β inhibitor) and obeticholic acid were administered to established iBHs from day 11 to day 21

respectively, followed by histologic analyses. As shown in HE staining images (Fig. 4), after treatment with TGF- β inhibitor or obeticholic acid for 10 days, pale cytoplasm of iBHs was reversed to red, which might be attributed to restoration of hepatocyte cytoskeleton and reduction of fat droplets. By contrast, phenotype of iBHs was not changed in dimethyl sulfoxide (DMSO) vehicle control group. These findings demonstrate that TGF- β inhibitor and obeticholic acid can improve histological appearance of iBHs independently, suggesting TGF- β and micro-cholestatics may play important roles in iBH formation.

TGF β 1 has been reported to participate in NASH through regulation of cell death and lipid metabolism [10]. Micro-cholestatics has been reported to be present in NASH liver [24], but what a role that micro-cholestatics plays in NASH is not clear. Furthermore, what is the relevance between TGF- β and micro-cholestatics in the current model and how do they participate in hepatocellular ballooning need to be further studied.

In summary, this study provides the first comprehensive analysis of liver-specific functions in BHs *in vitro* to date. Compared to normal hepatocytes, iBHs showed unaffected albumin secretion, reduced urea synthesis/CYP activities and loss of bile canaliculi, which might be explained by ER stress, mitochondrial dysfunction and fibrosis microenvironment. These findings correspond to clinical studies of human NASH. In addition, treatment with TGF- β inhibitor or obeticholic acid ameliorated the histological appearance of established iBHs, suggesting TGF- β and micro-cholestatics may be involved in iBH formation. Finally, this study demonstrates the priority of iBHs in mimicking not only morphological but also clinically relevant hepatic

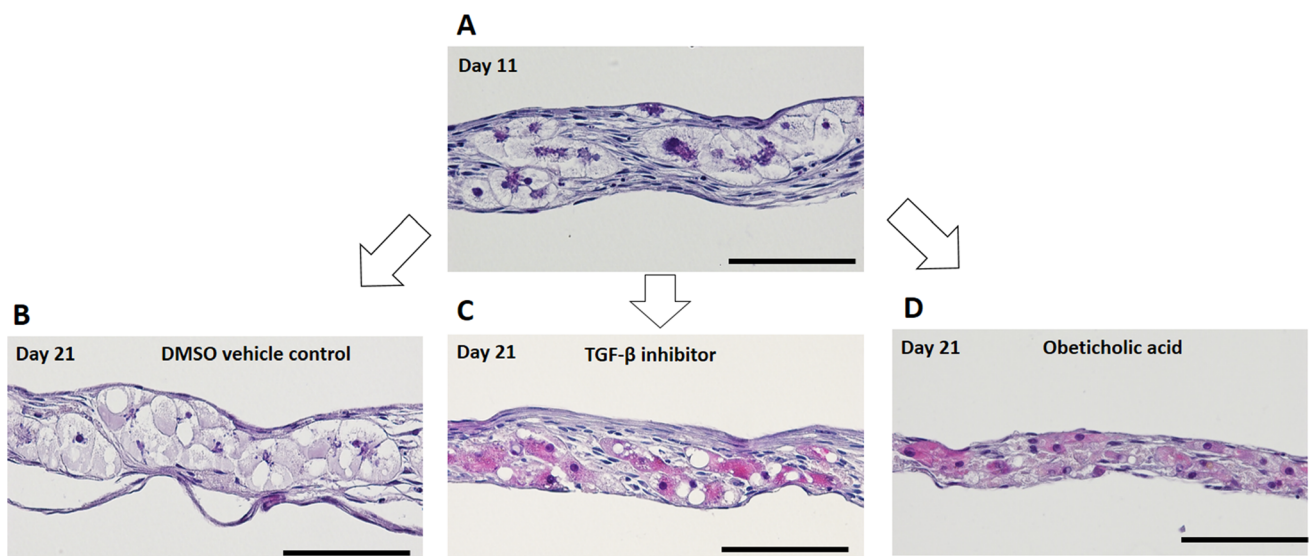


Fig. 4 Histological changes of iBHs in PHH/NHDF cell sheets after administration of 10 μ M TGF- β inhibitor (SB505124) or 10 μ M obeticholic acid for 10 days. Representative HE staining images of

A PHH/NHDF cell sheets on day 11, **B** DMSO vehicle control on day 21, **C** TGF- β inhibitor treated on day 21, and **D** obeticholic acid treated on day 21 were shown. Scale bar represents 100 μ m

dysfunctions in human NASH and may provide initial insight into development of *in vitro* NASH model.

Acknowledgements This work is supported by Adaptable and Seamless Technology Transfer Program through Target-Driven Research and Development (Grant No. JP18im0302706) from Japan Agency for Medical Research and Development (AMED), Hundred Talents Program of Guangdong Academy of Sciences (Grant No. 2020GDASYL-20200102005) and Innovation Ability Construction program of Guangdong Medical Device Research Institute (Grant No. 2017GDASCX-0103).

Compliance with ethical standards

Conflict of interest Tatsuya Shimizu is a member of the scientific advisory board and a stakeholder of CellSeed Inc. Tetsuya Ogawa, Yuki Kagawa and Hirotugu Kubo are employees of Nihon Kohden Corporation. Tokyo Women's Medical University was receiving research funds from CellSeed Inc. and Nihon Kohden Corporation.

Ethical statement There are no animal experiments carried out for this article.

References

1. Younossi ZM, Koenig AB, Abdelatif D, Fazel Y, Henry L, Wymer M. Global epidemiology of nonalcoholic fatty liver disease-meta-analytic assessment of prevalence, incidence, and outcomes. *Hepatology*. 2016;64:73–84.
2. Williams CD, Stengel J, Asike MI, Torres DM, Shaw J, Contreras M, et al. Prevalence of nonalcoholic fatty liver disease and nonalcoholic steatohepatitis among a largely middle-aged population utilizing ultrasound and liver biopsy: a prospective study. *Gastroenterology*. 2011;140:124–31.
3. Farrell GC, Wong VW, Chitturi S. NAFLD in Asia-as common and important as in the West. *Nat Rev Gastroenterol Hepatol*. 2013;10:307–18.
4. Thomsen KL, Grønbaek H, Glavind E, Hebbard L, Jessen N, Clouston A, et al. Experimental nonalcoholic steatohepatitis compromises ureagenesis, an essential hepatic metabolic function. *Am J Physiol Gastrointest Liver Physiol*. 2014;307:G295–301.
5. Appleby RN, Moghul I, Khan S, Yee M, Manousou P, Neal TD, et al. Non-alcoholic fatty liver disease is associated with dysregulated bile acid synthesis and diarrhea: a prospective observational study. *PLoS One*. 2019;14:e0211348.
6. Mouzaki M, Wang AY, Bandsma R, Comelli EM, Arendt BM, Zhang L, et al. Bile acids and dysbiosis in non-alcoholic fatty liver disease. *PLoS One*. 2016;11:e0151829.
7. Woolsey SJ, Mansell SE, Kim RB, Tirona RG, Beaton MD. CYP3A activity and expression in nonalcoholic fatty liver disease. *Drug Metab Dispos*. 2015;43:1484–90.
8. Yu Y, Ananthanarayanan A, Singh NH, Hong X, Sakban RB, Mittal N, et al. TGFβ1-mediated suppression of cytochrome P450(CYP) induction responses in rat hepatocyte-fibroblast co-cultures. *Toxicol In Vitro*. 2018;50:47–53.
9. Schuster N, Kriegelstein K. Mechanisms of TGF-beta-mediated apoptosis. *Cell Tissue Res*. 2002;307:1–14.
10. Yang L, Roh YS, Song J, Zhang B, Liu C, Loomba R, et al. Transforming growth factor beta signaling in hepatocytes participates in steatohepatitis through regulation of cell death and lipid metabolism in mice. *Hepatology*. 2014;59:483–95.
11. Charlton M, Sreekumar R, Rasmussen D, Lindor K, Nair KS. Apolipoprotein synthesis in nonalcoholic steatohepatitis. *Hepatology*. 2002;35:898–904.
12. Guy CD, Suzuki A, Zdanowicz M, Abdelmalek MF, Burchette J, Unalp A, et al. Hedgehog pathway activation parallels histologic severity of injury and fibrosis in human non-alcoholic fatty liver disease. *Hepatology*. 2012;55:1711–21.
13. Syn WK, Choi SS, Liaskou E, Karaca GF, Agboola KM, Oo YH, et al. Osteopontin is induced by hedgehog pathway activation and promotes fibrosis progression in nonalcoholic steatohepatitis. *Hepatology*. 2011;53:106–15.
14. Caldwell S, Ikura Y, Dias D, Isomoto K, Yabu A, Moskaluk C, et al. Hepatocellular ballooning in NASH. *J Hepatol*. 2010;53:719–23.
15. Matteoni CA, Younossi ZM, Gramlich T, Boparai N, Liu YC, McCullough AJ. Nonalcoholic fatty liver disease: a spectrum of clinical and pathological severity. *Gastroenterology*. 1999;116:1413–9.
16. Guy CD, Suzuki A, Abdelmalek MF, Burchette JL, Diehl AM. Treatment response in the PIVENS trial is associated with decreased Hedgehog pathway activity. *Hepatology*. 2015;61:98–107.
17. Brunt EM, Kleiner DE, Wilson LA, Belt P, Neuschwander-Tetri BA. NASH Clinical Research Network (CRN). Nonalcoholic fatty liver disease (NAFLD) activity score and the histopathologic diagnosis in NAFLD: distinct clinicopathologic meanings. *Hepatology*. 2011;53:810–20.
18. Matsuda N, Shimizu T, Yamato M, Okano T. Tissue engineering based on cell sheet technology. *Adv Mater*. 2007;19:3089–99.
19. Haraguchi Y, Shimizu T, Sasagawa T, Sekine H, Sakaguchi K, Kikuchi T, et al. Fabrication of functional three-dimensional tissues by stacking cell sheets in vitro. *Nat Protoc*. 2012;7:850–8.
20. Gao B, Sakaguchi K, Matsuura K, Ogawa T, Kagawa Y, Kubo H, et al. In vitro production of human ballooned hepatocytes in a cell sheet-based three-dimensional model. *Tissue Eng Part A*. 2020;26:93–101.
21. Khetani SR, Szulgit G, Del Rio JA, Barlow C, Bhatia SN. Exploring interactions between rat hepatocytes and non-parenchymal cells using gene expression profiling. *Hepatology*. 2004;40:545–54.
22. Khetani SR, Bhatia SN. Microscale culture of human liver cells for drug development. *Nat Biotechnol*. 2008;26:120–6.
23. Davidson MD, Kukla DA, Khetani SR. Microengineered cultures containing human hepatic stellate cells and hepatocytes for drug development. *Integr Biol (Camb)*. 2017;9:662–77.
24. Khetani SR, Chen AA, Ranscht B, Bhatia SN. T-cadherin modulates hepatocyte functions in vitro. *FASEB J*. 2008;22:3768–75.
25. Shaheen A. Effect of the unfolded protein response on ER protein export: a potential new mechanism to relieve ER stress. *Cell Stress Chaperones*. 2018;23:797–806.
26. Bartalena L, Robbins J. Effect of tunicamycin and monensin on secretion of thyroxine-binding globulin by cultured human hepatoma (Hep G2) cells. *J Biol Chem*. 1984;259:13610–4.
27. Ota T, Gayet C, Ginsberg HN. Inhibition of apolipoprotein B100 secretion by lipid-induced hepatic endoplasmic reticulum stress in rodents. *J Clin Invest*. 2008;118:316–32.
28. De Chiara F, Heebøll S, Marrone G, Montoliu C, Hamilton-Dutoit S, Ferrandez A, et al. Urea cycle dysregulation in non-alcoholic fatty liver disease. *J Hepatol*. 2018;69:905–15.
29. Fisher CD, Lickteig AJ, Augustine LM, Ranger-Moore J, Jackson JP, Ferguson SS, et al. Hepatic cytochrome P450 enzyme alterations in humans with progressive stages of nonalcoholic fatty liver disease. *Drug Metab Dispos*. 2009;37:2087–94.
30. Abdel-Razzak Z, Corcos L, Fautrel A, Champion JP, Guillouzo A. Transforming growth factor-beta 1 down-regulates basal and polycyclic aromatic hydrocarbon-induced cytochromes P-450

- 1A1 and 1A2 in adult human hepatocytes in primary culture. *Mol Pharmacol.* 1994;46:1100–10.
31. Segovia-Miranda F, Morales-Navarrete H, Kücken M, Moser V, Seifert S, Repnik U, et al. Three-dimensional spatially resolved geometrical and functional models of human liver tissue reveal new aspects of NAFLD progression. *Nat Med.* 2019;25:1885–93.
32. Younossi ZM, Ratziu V, Loomba R, Rinella M, Anstee QM, Goodman Z, et al. Obeticholic acid for the treatment of non-alcoholic steatohepatitis: interim analysis from a multicentre, randomised, placebo-controlled phase 3 trial. *Lancet.* 2019;394:2184–96.

Publisher's Note Springer Nature remains neutral with regard to jurisdictional claims in published maps and institutional affiliations.